Research Square

Preprints are preliminary reports that have not undergone peer review.
They should not be considered conclusive, used to inform clinical practice,
or referenced by the media as validated information.

Waterproof resistive random-access memory using a polyurethane-based liquid bandage for skin-attachable healthcare devices

Young Wook Kim
Yonsei University
Min Seong Kim
Yonsei University
Hyun Jae Kim
hjk3@yonsei.ac.kr

Yonsei University

Article

Keywords: liquid bandage, resistive random-access memory, solution process, waterproof

Posted Date: November 13th, 2026

DOI: https://doi.org/10.21203/rs.3.rs-11560474/v1

License: This work is licensed under a Creative Commons Attribution 4.0 International License.
Read Full License

Additional Declarations: No competing interests reported.

Waterproof resistive random-access memory using a polyurethane-based liquid bandage for skin-attachable healthcare devices

A polyurethane-based liquid bandage (LB) is proposed as an organic switching material for resistive random-access memory (ReRAM) in skin-attachable healthcare devices. LB is a commercially available liquid pharmaceutical product that forms a protective, water-resistant layer over wounds on human skin. LB-based ReRAM devices were fabricated using a solution process and exhibited bipolar resistive switching behavior. At a read voltage of 0.5 V, the devices exhibited a high resistance state (HRS) to low resistance state (LRS) resistance ratio of 7.73×10^3. Furthermore, the devices maintained stable switching performance without significant degradation over 100 consecutive switching cycles in deionized water, even without a passivation layer. Various analyses indicated that the resistive switching mechanism was associated with an oxidized Al layer formed between the LB thin-film and the top electrode. These results demonstrate the potential of LB as an organic switching layer for ReRAM devices.

Keywords: liquid bandage, resistive random-access memory, solution process, waterproof.

1. Introduction

Nowadays, improvements in quality of life have increased interest in better medical care and demand for personalized medical devices. Therefore, interest in body attachable devices for real time bio-signal monitoring has increased. Studies on devices attachable to human skin without physical discomfort have been actively conducted; these skin-attachable healthcare devices need to integrate data storage with biosignal detectors for real-time monitoring of the user's health. [1] Thus, nonvolatile memory is an essential component in skin-attachable healthcare devices. Various nonvolatile memory technologies have been proposed, such as resistive random access memory (ReRAM), phase-change random-access memory (PCRAM), and magnetoresistive random-access memory (MRAM). Of these, ReRAM has attracted particular attention because of its distinct advantages, such as faster switching speeds compared to PCRAM and a simpler cell structure than MRAM. It also has advantages including low manufacturing cost and low power consumption. [2-6] In display electronics, nonvolatile memory devices can be used to retain driving parameters without continuous power supply, which may reduce the need for repeated data loading during operation. [7] These advantages are beneficial for the application of ReRAM in skin-attachable healthcare devices, as ReRAM devices can be manufactured using relatively simple fabrication processes and operate with low power consumption, enabling longer operating times.

For practical applications of ReRAM in skin-attachable healthcare devices, ReRAM devices need to be flexible, lightweight, and conformable. However, inorganic materials are brittle and rigid, making them unsuitable for skin-attachable healthcare devices. [8-10] In particular, silicon used in conventional memory devices requires high temperature fabrication processes. To overcome these limitations, many alternative materials have been studied, and organic-based ReRAM devices are attractive

candidates. [11-15] However, organic-based ReRAMs are sensitive to external environmental factors. In particular, moisture, which is present in the environment or is a component of body fluids, can damage organic materials and degrade the performance of organic based ReRAM devices. Therefore, it is important to ensure resistance to moisture before applying organic-based ReRAM devices to skin-attachable healthcare devices.

In this regard, a polyurethane-based liquid bandage (LB), an organic material applicable to skin-attachable healthcare devices, was employed as a switching layer in ReRAM devices. LB is a commercial liquid-type pharmaceutical product used as a transparent bandage to cover wounds on human skin owing to its biocompatibility, water-resistance, and flexibility. We fabricated LB-based ReRAM devices at a low temperature (80^{o}C) using a solution process and evaluated their resistive switching characteristics. Furthermore, after immersion in deionized (DI) water, the electrical characteristics of LB-based ReRAM devices were evaluated to confirm its water-resistance property. Finally, various analyses were performed to verify the resistive switching mechanism of LB-based ReRAM devices.

2. Experimental

Fabrication process

Figure 1 shows a schematic illustration of the LB-based ReRAM fabrication process. We used a heavily doped p-type silicon (p^{+}-Si) substrate as the bottom electrode. The substrate was cut into 2 × 2 cm pieces and cleaned in acetone, methanol, and DI water for 10 min each respectively. A diluted LB (Mundipharma Korea) solution was prepared by mixing LB with ethanol at a volume ratio of 1:6 (LB:ethanol). The LB thin film was deposited onto the cleaned substrate by spin coating at 3000 rpm for 30

s. Subsequently, the sample was annealed in ambient air for 10 min at 80°C. Finally, an aluminum (Al) top electrode was deposited onto the LB thin film by electron beam evaporation through a shadow mask.

Measurement and Analysis

The electrical characteristics of the LB-based ReRAM were measured using a dark probe station equipped with a parameter analyzer (Model 4200A, Keithley Instruments). The microstructure of the LB-based ReRAM was analyzed using transmission electron microscopy (TEM; Model JEM-F200, JEOL Ltd.). The composition of the LB-based ReRAM was analyzed by X-ray photoelectron spectroscopy (XPS) depth profiling and counts per second (CPS) scan profiling (Model K-alpha, Thermo Fisher Scientific).

3. Result and discussion

Figure 2a shows the resistive switching characteristics of LB-based ReRAM. The bottom electrode, p^+-Si, was grounded; a voltage sweep from positive to negative bias was applied to the top electrode. ReRAM operates through changes in the resistance associated with conductive filaments. It switches to the low resistance state (LRS) under a set voltage bias, while it switches to the high resistance state (HRS) under a reset voltage bias. Herein, the set voltage induces the transition from HRS to LRS and the reset voltage induces the transition from LRS to HRS. The LB-based ReRAM exhibited bipolar resistive switching behavior, with a set voltage of 2.45 V and a reset voltage of –2.30 V in the first cycle. Moreover, LB-based ReRAM maintained stable switching performance over 100 consecutive cycles. The LB-based ReRAM exhibited an HRS/LRS resistance ratio of 7.73×10^3 at a read voltage of 0.5 V. Based on these switching results, the potential of LB-based ReRAM as a nonvolatile memory device was demonstrated. As shown in **Figure 2b**, we investigated the current voltage

characteristics using linear fitting to investigate the resistive switching mechanism of LB-based ReRAM. **Figure 2b** presents a double-logarithmic plot of the positive voltage region of **Figure 2a** to further investigate the resistive switching mechanism of LB-based ReRAM. The numbers indicated in **Figure 2b** represent the fitted slope values. In the LRS, the fitting result indicated ohmic conduction (slope ≈ 1) suggesting a linear relationship between current and voltage. The slope in the HRS changes from 1 to 2 and 3 as the voltage increases, suggesting trap controlled space charge limited current conduction. Moreover, LB-based ReRAM showed a sharp increase in current at the set voltage. This conduction behavior suggests that the resistive switching mechanism of the LB-based ReRAM involves the formation and rupture of localized conductive filaments near the interface. [16-17] Previous studies have investigated the resistive switching mechanisms of ReRAM devices based on organic insulating materials. [18-19] One possible origin of resistive switching is the native oxide layer formed at the interface between a metal electrode and an organic layer. Therefore, when Al, which is easily oxidized, is used as the top electrode of the LB-based ReRAM, it can react with oxygen containing functional groups, such as hydroxy group (−OH), in LB, leading to the formation of an AlO_x layer. [20-22]

We performed TEM imaging analysis and CPS line profile to verify the presence of the AlO_x layer formed at the interface between LB and Al top electrode. The TEM image shows that an AlO_x layer approximately 5 nm thick was formed at the interface between LB and Al, as shown in Figure 3a. Nevertheless, detecting with certainty the existence of a new layer created between the Al electrode and insulator layer was difficult in the dark field of the TEM image. Therefore, the CPS scan profile was analyzed along the line from a to a′ in Figure 3a to examine the distributions of carbon and oxygen. As shown in Figure 3b, the carbon signal was observed over the

range of 7 to 24 nm, while the oxygen signal began to increase at approximately 8 nm. Notably, the oxygen signal reached its maximum at approximately 18 nm. This result suggests the presence of an AlO_x layer near the 18 nm position. In addition, we conducted XPS depth profile analysis to obtain further evidence of the AlOx layer formed at the interface. Figure 4a shows the Al 2p XPS depth profile of LB-based ReRAM obtained by argon-ion etching from the Al electrode toward the LB thin film. The Al 2p spectra of LB-based ReRAM were deconvoluted into Al and Al-O peaks centered at 72.6 and 74.6 eV, respectively. [23-25] As etching progressed toward the LB thin-film, the Al-O peak gradually increased in intensity. The TEM images, CPS line profile, and XPS depth profile results collectively support the presence of an AlOx layer at the interface between LB and Al. As a result, based on various analyses we verified that the resistive switching mechanism of LB-based ReRaMs is due to the AlOx layer. **Figure 5** shows a schematic illustration of the resistive switching mechanism. In the initial state, the presence of the AlO_x layer at the interface between LB and Al restricts current flow, resulting in an HRS. When a positive voltage is applied to the LB-based ReRAM, oxygen ions in the AlO_x layer move toward the upper interface, leading to the formation of highly conductive oxygen vacancy (V_o) filaments and the device switches to the LRS. When a negative voltage is applied to the LB-based ReRAM, oxygen ions move downward to fill V_o; the conductive filaments rupture, causing the device to return to the HRS.

Finally, to evaluate the potential applicability of LB-based ReRAM to healthcare devices, water-resistance tests were conducted on the LB thin film and LB-based ReRAM devices. As shown in **Figure 6a**, the LB thin-film showed no visible changes after immersion in DI water for 2 weeks. **Figure 6b** shows a schematic illustration of the measurement setup used to evaluate the switching characteristics of

LB-based ReRAM in DI water. As shown in **Figure 6c**, LB-based ReRAM exhibited bipolar resistive switching behavior with an HRS/LRS resistance ratio of approximately 10^2 in the first cycle at a read voltage of 0.5 V. Moreover, the LB-based ReRAM maintained stable resistive switching behavior over 100 consecutive switching cycles. These results were consistent with the immersion test results, which showed no visible changes in the LB thin film. LB demonstrated water-resistance, suggesting its potential as a switching layer material in ReRAM devices for skin-attachable healthcare devices.

4. Conclusion

We successfully demonstrated the potential of LB as a switching layer material in ReRAM devices for data storage applications in healthcare devices. The LB-based ReRAM exhibited bipolar resistive switching behavior and maintained stable switching performance over 100 consecutive cycles without significant degradation. TEM image, CPS line profile analysis, and XPS depth profile analysis indicated that the resistive switching mechanism of LB-based ReRAM was associated with an AlO_x layer formed at the interface between LB and Al. Furthermore, the LB-based ReRAM maintained stable resistive switching behavior during the water-resistance test in DI water. The low-temperature solution process and water-resistant switching characteristics may also provide a basis for further investigation of organic memory devices for display electronics. These findings highlight the potential of LB-based ReRAM for skin-attachable biocompatible electronics.

5. Reference

[1] J. Chen, H. Ding, X. Sheng, J. Inf. Disp., 25, 1-12 (2024). https://doi.org/10.1080/15980316.2023.2248403

[2] R. Waser, R. Dittmann, G. Staikov, K. Szot, Adv. Mater., 21, 2632 (2009). https://doi.org/10.1002/adma.200900375

[3] H. Wang, X. Yan, Phys. Status Solidi RRL, 13, 1900073 (2019). https://doi.org/10.1002/pssr.201900073

[4] A. Chavent, P. Coelho, J. Chatterjee, N. Strelkov, S. Auffret, L. Buda-Prejbeanu, R. Sousa, L. Vila, L. Prejbeanu, B. Diény, C. Baraduc, ACS Appl. Electron. Mater., 3, 2607 (2021). https://doi.org/10.1021/acsaelm.1c00198

[5] A. K. Ramesh, K. M. Chen, Y. J. Lin, P. Singh, J. H. Wei, Y. C. Hsin, C. I. Wu, Y. C. Tseng, ACS Appl. Electron. Mater., 3, 4047 (2021). https://doi.org/10.1021/acsaelm.1c00554

[6] M. Ahn, J. S. Oh, D. Park, H. Jung, S. Park, K. Jeong, D. Kim, N. E. Sung, K. S. Lee, C. W. Yang, M. H. Cho, ACS Appl. Electron. Mater., 2, 2418 (2020). https://doi.org/10.1021/acsaelm.0c00370

[7] C. H. Shin, O. K. Kwon, J. Soc. Inf. Disp., 17, 481-487 (2009). https://doi.org/10.1889/JSID17.5.481

[8] Y. J. Tak, S. P. Park, T. S. Jung, H. Lee, W.-G. Kim, J. W. Park, H. J. Kim, J. Inf. Disp., 17, 73 (2016). https://doi.org/10.1021/acsaelm.0c00370

[9] Q.-D. Ling, D.-J. Liaw, C. Zhu, D. S.-H. Chan, E.-T. Kang, K.-G. Neoh, Prog. Polym. Sci., 33, 917 (2008). https://doi.org/10.1016/j.progpolymsci.2008.08.001

[10] H. Lee, K. S. Chang, Y. J. Tak, T. S. Jung, J. W. Park, W.-G. Kim, J. Chung, C. B. Jeong, H. J. Kim, J. Inf. Disp., 18, 131 (2017). https://doi.org/10.1080/15980316.2017.1322152

[11] N. R. Hosseini, J. S. Lee, Adv. Funct. Mater., 25, 5586 (2015). https://doi.org/10.1002/adfm.201502592

[12] H. Wang, B. Zhu, X. Ma, Y. Hao, X. Chen, Small, 12, 2715 (2016). https://doi.org/10.1002/smll.201502906

[13] H. Wang, F. Meng, Y. Cai, L. Zheng, Y. Li, Y. Liu, Y. Jiang, X. Wang, X. Chen, Adv. Mater., 25, 5498 (2013). https://doi.org/10.1002/adma.201301983

[14] X. He, J. Zhang, W. Wang, W. Xuan, X. Wang, Q. Zhang, C. G. Smith, J. Luo, ACS Appl. Mater. Interfaces, 8, 10954 (2016). https://doi.org/10.1021/acsami.5b10414

[15] S.C. Jang, J. Shim, H. Jang, Y. Lee, S. Biswas, J. Park, H. Shin, H. Kim, S. Kim, H. S. Kim, J. Inf. Disp., 26, 341-356 (2025). https://doi.org/10.1080/15980316.2025.2548808

[16] Y. C. Yang, F. Pan, Q. Liu, M. Liu, F. Zeng, Nano Lett., 9, 1636 (2009). https://doi.org/10.1021/nl900006g

[17] M.-J. Lee, S. Han, S. H. Jeon, B. H. Park, B. S. Kang, S.-E. Ahn, K. H. Kim, C. B. Lee, C. J. Kim, I.-K. Yoo, Nano Lett., 9, 1476 (2009). https://doi.org/10.1021/nl803387q

[18] J. Choi, J.-S. Kim, I. Hwang, S. Hong, S. Jeon, S.-O. Kang, B. Park, D. Kim, M. Lee, S. Seo, Appl. Phys. Lett., 95, 022109 (2009). https://doi.org/10.1063/1.3173813

[19] S. K. Kim, J. Y. Kim, S.-Y. Choi, J. Y. Lee, H. Y. Jeong, Adv. Funct. Mater., 25, 6710 (2015). https://doi.org/10.1002/adfm.201502734

[20] A. Sawa, Mater. Today, 11, 28 (2008). https://doi.org/10.1016/S1369-7021(08)70119-6

[21] M. Cölle, M. Büchel, D. M. de Leeuw, Org. Electron., 7, 305 (2006). https://doi.org/10.1016/j.orgel.2006.03.014

[22] Y. Zhang, H. Wu, Y. Bai, A. Chen, Z. Yu, J. Zhang, H. Qian, Appl. Phys. Lett., 102, 233502 (2013). https://doi.org/10.1063/1.4810000

[23] S. Schoser, G. Bräuchle, J. Forget, K. Kohlhof, T. Weber, J. Voigt, B. Rauschenbach, Surf. Coat. Technol., 103–104, 222 (1998). https://doi.org/10.1016/S0257-8972(98)00397-1

[24] B. Yan, S. Liu, Y. Heng, Y. Yang, Y. Yu, K. Wen, Nanoscale Res. Lett., 12, 363 (2017). https://doi.org/10.1186/s11671-017-2131-8

[25] S. J. Heo, D. H. Yoon, T. S. Jung, H. J. Kim, J. Inf. Disp., 14, 79 (2013). https://doi.org/10.1080/15980316.2013.806274

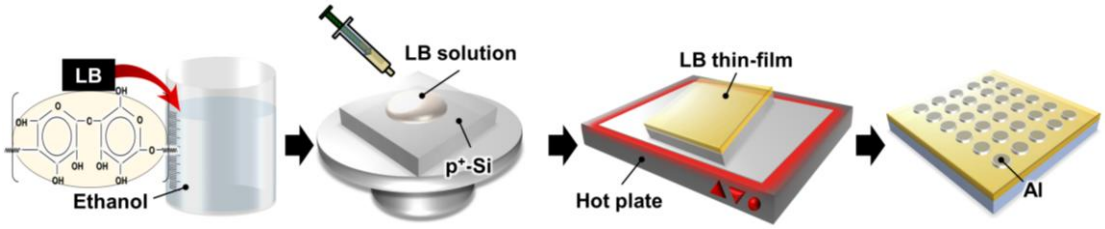


Figure 1. Schematic illustration of the fabrication process for a liquid bandage (LB)-based resistive random-access memory (ReRAM).

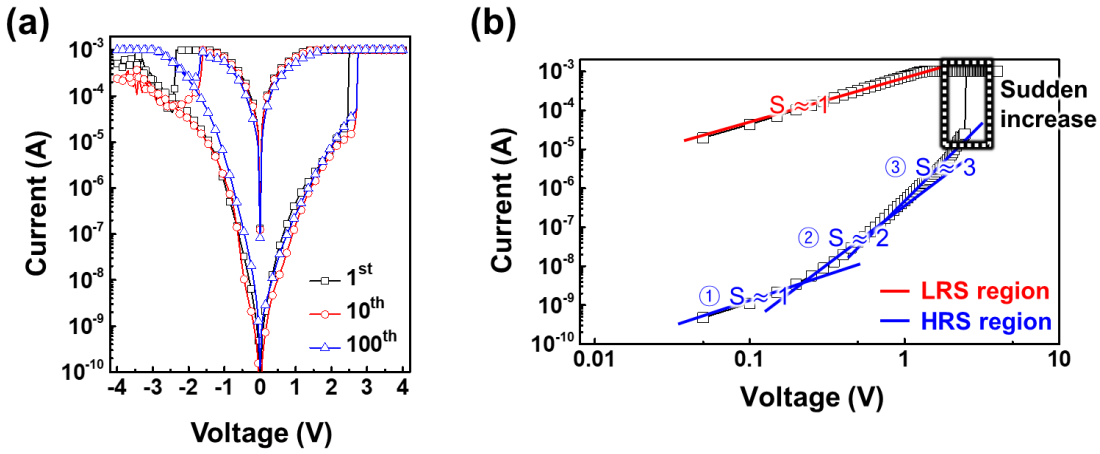


Figure 2. Resistive switching characteristic of LB-based ReRAM (a) I-V characteristics over 100 consecutive cycles and (b) double logarithmic fitting of the I-V characteristics.

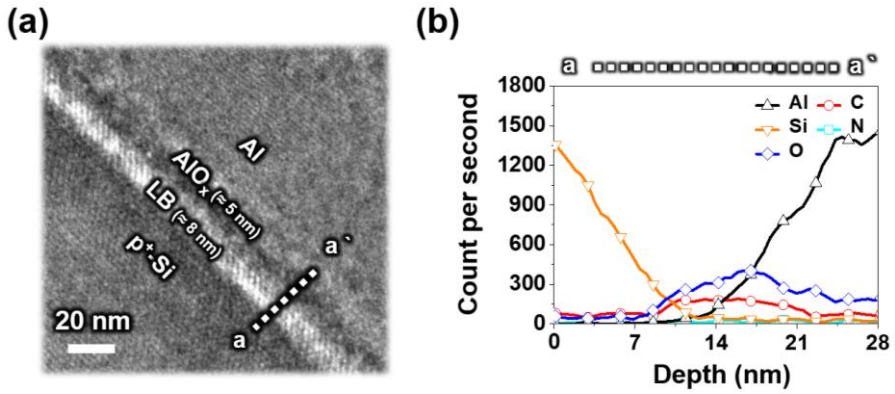


Figure 3. Structural and compositional analyses of LB-based ReRAM (a) TEM image and (b) CPS scan profile.

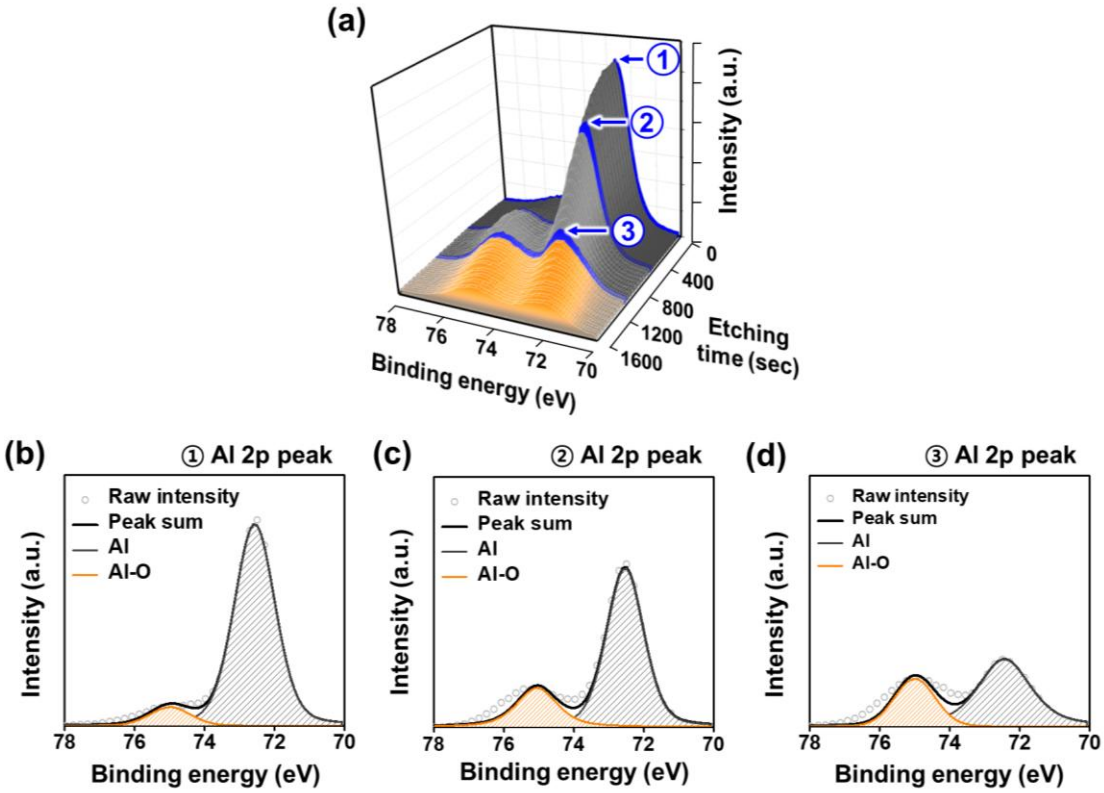


Figure 4. Al 2p XPS analysis of LB-based ReRAM (a) depth profile obtained by etching from the Al top electrode toward the LB thin film and deconvoluted Al 2p spectra at positions (b) ①, (c) ②, and (d) ③.

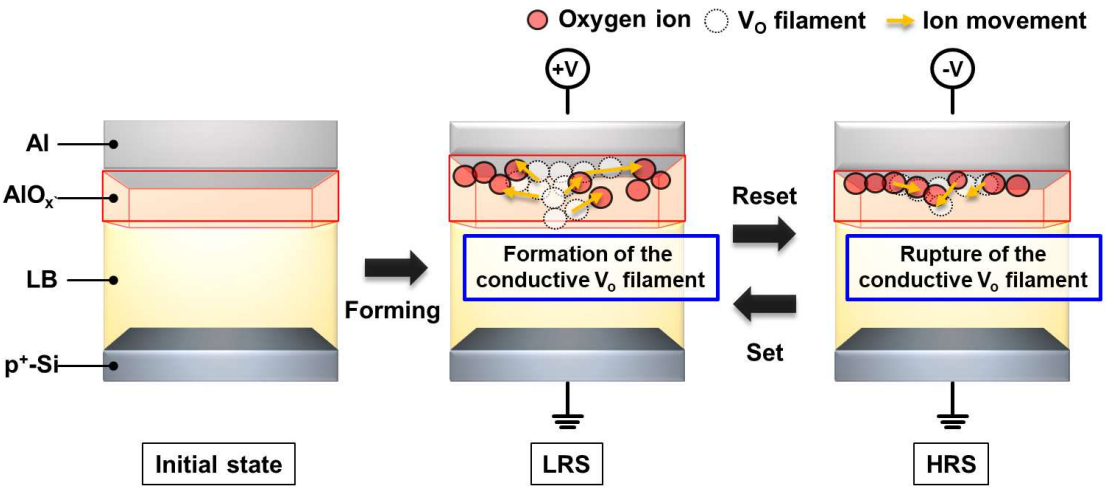


Figure 5. Schematic diagram of the switching mechanism for LB-based ReRAM.

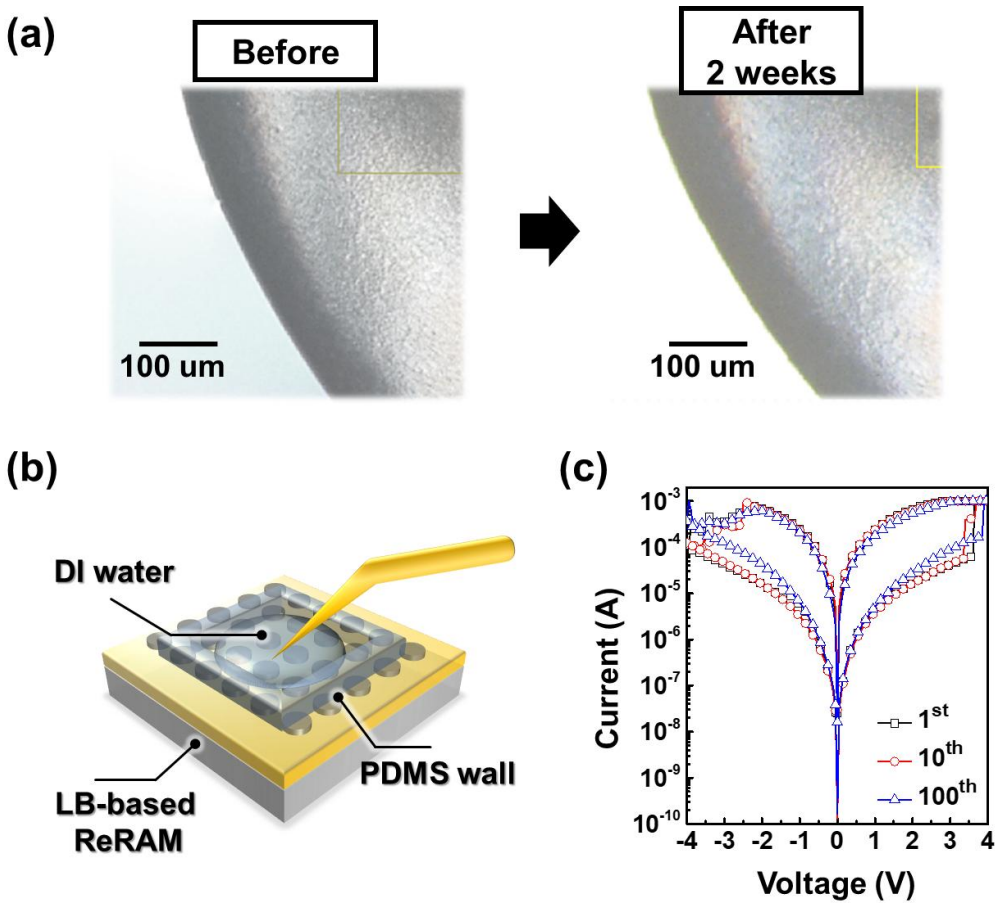


Figure 6. Water-resistance characteristics of LB-based ReRAM: (a) water-resistance test of the LB thin-film, (b) schematic diagram of the measurement setup for LB-based ReRAM in deionized (DI) water, and (c) I–V resistive switching characteristics of LB-based ReRAM during immersion in DI water.